

We are IntechOpen, the world's leading publisher of Open Access books Built by scientists, for scientists

4,800

Open access books available

122,000

International authors and editors

135M

Downloads

Our authors are among the

154

Countries delivered to

TOP 1%

most cited scientists

12.2%

Contributors from top 500 universities



WEB OF SCIENCE™

Selection of our books indexed in the Book Citation Index
in Web of Science™ Core Collection (BKCI)

Interested in publishing with us?
Contact book.department@intechopen.com

Numbers displayed above are based on latest data collected.
For more information visit www.intechopen.com



Trace Elements in Hair: Relevance to Air Pollution

Jun-ichi Chikawa, Jeremy Salter, Hiroki Shima,
Takaaki Tsuchida, Takashi Ueda,
Kousaku Yamada and Shingo Yamamoto

Additional information is available at the end of the chapter

<http://dx.doi.org/10.5772/intechopen.74373>

Abstract

Elemental concentrations of single hair samples taken from 2003 to 2012 had been evaluated by X-ray fluorescence for the assessment of the relation between calcium and cancer. Early results implied a mechanism linking hair and serum element concentrations with a shift in element levels over time. After 2009, pollution-attributable differences were seen in the levels of Ca, Sr, P, Cl, Br, K, S, elements under renal control by parathyroid hormone (PTH), as well as Cu, Zn, Ti. Especially, hair taken from February to March 2011 showed low [Cu] and [Zn] indicating about half of the normal serum level and often three orders of magnitude higher [Ti] than typical. These specimens also showed higher serum [S] than usual, and except for one patient with PTH-related disease, all the subjects had the normal or lower hair calcium than typical for earlier years. Almost all the subjects showed store-operated Ca channel gating. The pollution era is associated with an increase in hair Na, a decrease in K, and abnormally low P, suggesting a functional deterioration of Na⁺/K⁺-ATPase. These results can be attributed to increases in serum Ca and S coincident with breathing the polluted air; the incorporated Ca closes the ion channels of hair matrix cells but may be moved with P to bone, resulting in the abnormal P deficiency, likely producing an ATP shortage in serum. This insufficient ATP supply may result in inactivated molecular pumps and hypokalemia contributing to fatal ventricular fibrillation in patients with myocardial infarction. The pollution increase [S] in serum may be excreted by forming sulfide compounds with Cu and Zn, resulting in Cu deficiency necessary for making elastin to repair damage in blood vessels. The K and Cu deficiencies observed appear to account for the reported increase in infarction mortality after high-pollution days.

Keywords: calcium, sulfur, ion channels, parathyroid hormone, Na⁺/K⁺-ATPase, hypokalemia, yellow haze, copper, zinc

1. Introduction

Synchrotron X-ray fluorescence analysis of single hair segments was achieved by Iida and Noma [1]. Today, elemental distribution in hair microstructures has been observed especially in cosmetic studies [2] and occasionally in environmental studies [3]. In our previous work [4–6], the study of the relations between elemental concentrations in serum and hair (total concentration instead of structural distribution) was employed for our inquiries into links between cancer and calcium metabolism. X-ray fluorescence (XRF) detects many elements, and in time it became clear that the spectra acquired for cancer assessment also showed pollution-related trends.

Pollution particles smaller than 10 and 2.5 μm suspended in the atmosphere are referred to as “PM 10” and “PM 2.5” (fine Particulate Matter). An association between daily mean PM concentration and daily mortality was shown by a statistical model [7–10]. Also, correlations between PM and cancer were investigated [9]. The PM 2.5 is mainly attributed to soot particles contained in gas emissions from diesel vehicles and manufacturing facilities and contains various substances; combustion-associated gases include sulfur and nitrogen oxides. The PM includes wind-blown yellow sand that often comes to Japan [10] by desertification in the continent. Such particulates have reached California, British Columbia, and the French Alps [11–14]. Today, air pollution PM 2.5 is a universal problem, routinely affecting most of the world, although most obvious in and downwind of industrial areas. PM 2.5 is too small to be filtered by the conventional gauze mask and can deposit materials in capillary vessels in the lung [15].

In this study, to explore the possible origins of the mortality increase observed among cardiac patients, elemental inflow from polluted air into blood has been investigated by review of X-ray fluorescence analyses (XFA) of hair using the ratio of characteristic X-ray peaks to background scatter [4–6]. Since the scatter is a function of the mass of the sample within the beam, the peak-to-scatter ratio (P/S) can be used as a unitless relative concentration of each detected element, independent of hair thickness and shape. With the relationships of serum and hair elements given by the equations in **Table 1** previously established [5], we obtained useful approximations of element levels in serum.

XFA for scalp hair has revealed ion channel gating of hair matrix (HM) cells [4]. By the principle of “inflow-outflow equality,” the content of an element in growing hair must be equal to the inflow into the HM cells from blood [4, 5], and the elements admitted through ion channels occur in hair at two distinct levels produced by the closing or opening (gating) of the relevant channels (in vivo). By such channel gating, homeostasis of cellular essential elements can be maintained. Especially, Ca is an overall regulator of ion gating. We had given ten subjects 2-week oral calcium supplementation; the (dried) serum samples showed a single value for Ca [5]. Similarly, no significant variation was seen among the subjects for Sr, Cl, Br, K, S, and P, elements under renal homeostatic control, although in nonsupplemented subjects, considerable variation is usual [4–6]. Calcium is the central player for the homeostatic control of the elements, and usually, therefore, store-operated Ca channels are activated to maintain

$[Fe]_S = [Fe]_P$	$[Fe]_H = [Fe]_P = 15$	(4)
$[Cu]_S = [Cu]_P$	$[Cu]_H = [Cu]_P = 20$	(5)
$[Zn]_S = [Zn]_P$	$[Zn]_H = [Zn]_P^2 = 400$	(6)
$[S]_P = [S]_I$	$[S]_{HC} = [S]_P = 20$	(7)
	$[S]_{HO} = (1/2)[S]_I^2 = 200$	(8)
$[Ca]_P = [Ca]_I$	$[Ca]_{HC} = [Ca]_P = 10$	(9)
	$[Ca]_{HO} = (1/2)[Ca]_I^2 = 50$	(10)
$[Sr]_P = [Sr]_I$	$[Sr]_{HC} = [Sr]_P = 10$	(11)
	$[Sr]_{HO} = (1/2)\{[Sr]_P + [Sr]_I\}^2 = 200$	(12)
$[Cl]_P = 0.04[Cl]_I$	$[Cl]_{HC} = [Cl]_P = 10$	(13)
	$[Cl]_{HO} = \{2[Cl]_I\}^{1/2} = 22$	(14)
$[Br]_P = 0.04[Br]_I$	$[Br]_{HC} = [Br]_P = 10$	(15)
	$[Br]_{HO} = \{2[Br]_I\}^{1/2} = 22$	(16)
$[K]_S = [K]_I$	$[K]_{HC} = 7.1[K]_S = 300$	(17)
$[P]_P = [P]_I = (1/4)[P]_S$	$[P]_{HC} \geq 10$	(18)
	$[P]_{HO} = 5 [P]_I^{1/2} = 5$	(19)

Numerical values of peak/scatter as apparent concentrations of element X defined by Eq. (2). Eq. (1): $[X]_S = [X]_I + [X]_P$. Subscripts: H = hair, S = serum, I = serum Ion, P = serum Protein, OH = Hair produced during Open ion channels, HC = Hair produced during Closed ion channels.

Dried serum was measured to be $[Na]_S = 10$ by the definition $[X] = P/S$ Eq. (2), and hair usually shows no Na peak, that is, $[Na]_H = 1$. This resulting ratio corresponds to established values: $[Na] = 142$ mmol/L in serum and $[Na] = 14$ mmol/L in cell [23]. The standard concentration $[X]_H$ given by Eq. (2), of course, can be converted into the conventional expression such as $[Ca]_{HC} = 0.49$ mg/g and $[Ca]_{HO} = 2.5$ mg/g [5].

Table 1. Standards of hair $[X]_H$ and dried serum $[X]_S$.

the normal intracellular $[Ca]$. Thus, hair elements constitute a record of the combination of serum elements and ion channel function.

The store-operated Ca channels on the plasma membrane are understood to open when Ca^{2+} stores are depleted at the endoplasmic reticulum (ER) [16–18]. “Store-operated ion channels” adjust the intracellular Ca ion level toward the normal, and an XFA scan along hair shows that the normal $[Ca]_{HC} = 10$ was maintained despite the ongoing channel gating revealed by the noted fluctuation in $[Sr]_H$ [6]. Therefore, the store-operated channels gate due to shortage of Ca stored in serum protein [5, 6], corresponding to hair Ca less than the normal ($[Ca]_{HC} < 10$ by Eq. (9) in **Table 1**).

However, when the serum Ca deficiency further proceeds beyond the range covered by the store-operated Ca entry (SOCE), the deficiency increases the secretion of parathyroid hormone (PTH), which causes PTH-activated Ca channel gating. Such channel activity is due to membrane voltage and propagates from channel to channel, resulting in the upper range $[Ca]_H > 10$

and reaching the maximum $[Ca]_{HO} = 50$ and $[Sr]_{HO} = 200$ [Eqs. (10) and (12) in **Table 1**]. Ca oral supplementation immediately transits this highest level into the normal or less than normal $[Ca]_{HC} \leq 10$ and $[Sr]_{HC} \leq 10$; PTH regulates the Ca channel(s) of HM cells [4–6]. As a typical example, de Groot et al. [19] elucidated the epithelial Ca channel TRPV-5 activated by PTH, which is responsible for Ca reabsorption in renal tubule [20]. Today, for utilizing the channel on-off action for biosensing applications, artificial cell membrane systems have been widely investigated [21].

Thus, calcium has a very high essentiality and homeostasis. The serum standard values for subjects with Ca supplementation are given in **Table 1**. The hair standards were calculated from the serum standards and confirmed by the *P/S* FXA [5, 6]. For this work, Ca may be treated as the major regulator of ion channels and may react to a change in serum Ca level in just 15–20 min [22].

Because sulfur-containing amino acids, methionine and cysteine are components of almost all protein molecules, sulfur has also high essentiality and homeostasis and is contained as the ionic sulfur species (SO_4^{2-}) in serum [23, 24]. Its relation between serum and hair is similar to that of Ca as seen from Eqs. (7)–(10) in **Table 1**, although the sulfate ion channels have not been reported to the knowledge of the authors [5].

We have observed elemental levels in the hair of thousands of people from 2003 to the present day. Samples after 2009 show significant changes in hair elements, and today the intrinsic hair element levels cannot be seen any more. However, the homeostasis of Ca and S is maintained even with their great inflow into serum from the polluted air at the sacrifice of other important elements responsible for heart activity, resulting in the increased mortality in myocardial infarction cases up to 7 days following short-term pollution [25–27].

2. Samples and method

All the hair and blood samples were collected after informed consent was obtained in accordance with the ethical standards of Hyogo College of Medicine.

X-ray fluorescence analysis (XFA) of the hair samples was carried out using synchrotron radiation at the Photon Factory's (PF) BL4A beamline in the same way as previously [4–6]: excitation energy was 17.4 keV (0.71 Å), the hair was suspended into the X-ray beam in vacuum, and fluorescence detected using a lithium-drifted silicon detector. Because almost all our subjects dye their hair, to avoid hair contamination, only dye-free fresh hair root (length about 1 mm) was used for single-point evaluation. Datum was typically collected for a minute in the range of 0.5–17.5 keV, and the fluorescence peaks evaluated on the log-scale plot by height, all k-alphas except the Ca K-beta peak at 4.0 keV used to avoid interferences. Since hair grows at about 1 cm per month, each data point corresponds to about 3 days of hair growth. The variation of concentrations with time in **Figure 1** was observed by scanning along hair strands using a beam width of 0.05 mm.

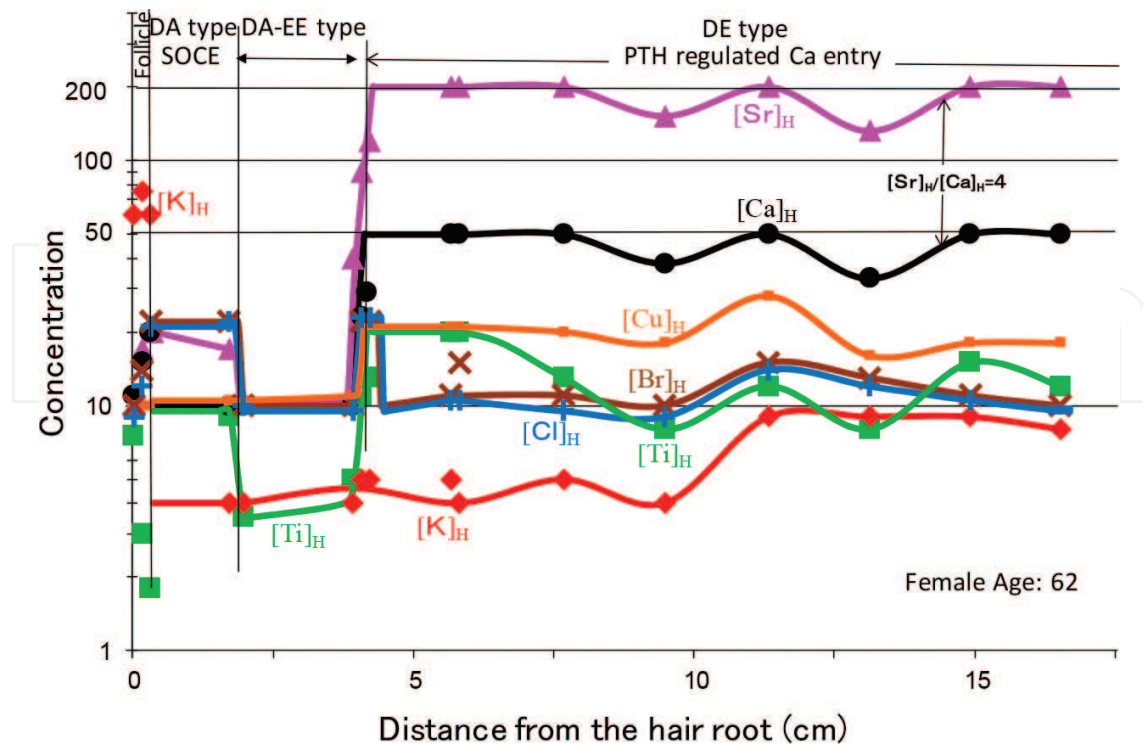


Figure 1. Typical Ca deficiency observed along a single hair strand by scanning 0.05-mm-width XFA. Transitions of DE type (PTH-regulated Ca entry), DA-EE type (Ca channel closing with a low $[K]_H$), and DA type (store-operated Ca entry, SOCE) can be seen with the $[Ca]_H$ variation due to the Ca channel gating, resulting in synchronized variations for $[Cu]_H$, $[Ti]_H$, $[K]_H$, $[Cl]_H$, and $[Br]_H$. In the SOCE region (DA type), $[Ti]_H$ and $[Sr]_H$ are still high, and other elements have the standard levels. Female subject age: 62.

3. Concentration relations between serum and hair

Serum contains water at 90–92% and Ca at 8.5–10.2 mg/dL; these Ca values correspond to 92 and 90% water contents, respectively, with negligible $[Ca]$ variations in dried serum. Dried serum is calculated to have Ca at 1 mg/g. Hair can be regarded as serum protein containing mineral elements. For example, Cu exists mainly not as free ions, only bound to serum protein, and the reported serum $[Cu]_S$ of 17 $\mu\text{mol/L}$ [28] becomes dried serum concentration of 207 $\mu\text{mol/kg}$, which is in good agreement with the reported hair Cu concentration of 190–200 $\mu\text{mol/kg}$. Therefore, any element in serum protein has about the same concentration in hair, if no ions flow into the hair.

In most cases, the total concentration of element X in dried serum, $[X]_S$, is the sum of

$$[X]_S = [X]_I + [X]_P \quad (1)$$

$[X]_I$ and $[X]_P$, the concentrations of ionic and protein-bound X, respectively. By the principle of the inflow-outflow equality, X's hair concentrations $[X]_H$ can occur in two levels depending on whether the ion channels for element X are gating or closing;

$[X]_{HO}$ = hair concentration in the case of the gating (open) ion channels.

$[X]_{HC}$ = hair concentration in the case of the closing ion channels.

For specimen mass M within the excitation X-ray beam in XFA, the peak height P for element X must be $P = kM[X]$, with k , a proportional constant, so $\log[X] = \log P - \log kM$. Logarithmic spectra for thick and thin specimens having the same concentration can be superimposed by moving one to the other vertically, that is, $\log kM = \log S$, and.

$$\log[X] = \log P - \log S = \log(P/S), \quad (2)$$

independently of the specimen thickness, where S is the background due to X-rays scattered by the specimen. Eq. (2) is valid even for thick specimens because the X-ray absorption occurs for P and S in the same way. (The hair was suspended in the X-ray beam in vacuum, so there is no other mass to contribute background scatter.) Using this definition for $[X]$, the relations between $[X]_H$ and $[X]_S$ obtained in the previous paper [5] are listed in **Table 1** (also, see **Figure 3**).

As seen from the foregoing argument, the background S is due to serum (hair) protein (nonprotein solids: 3–4%). According to the Gamble [23] gram, the ionic element species are controlled to maintain electric neutrality with $[\text{Protein}^-]$ in serum. Then, the ratio of the number of X atoms to the number of the protein molecules within the excitation X-ray beam in XFA, which is proportional to $[X] = P/S$, is under homeostatic control. If congener elements, X and Z , have a proportionality, we have $[X] = [Z]$ by the definition Eq. (2), as $[\text{Cl}]_H = [\text{Br}]_H$ in **Table 1**. The concentration by Eq. (2) can be considered to use the standard value of each element as a unit and results in a new concentration system to show the relationship of elements in dried serum, cell, and hair.

For an element Z such as Cu, Fe, and Zn being protein-bound and having no ion in serum, the value $\log[Z]_H = [\log P - \log S]_H$ is normalized for comparing their concentrations by.

$$\log[Z]_H = [\log P - \log S]_H / ([\log P - \log S]_{H, \text{st}}) \quad (3)$$

using the standard $([\log P - \log S]_{H, \text{st}})$ for hair. The standard values for the Ca-supplemented healthy subjects are $[\text{Cu}]_H = 20$, $[\text{Fe}]_H = 15$ and $[\text{Zn}]_H = 400$ (**Table 1**).

By the principle of “inflow-outflow equality,” hair composition reveals ion channel closing and opening. There may be many kinds of ion channels and receptors, some yet unknown. Though sulfate ion channels have not been reported, we observed upper $[S]_{HO}$ and lower $[S]_{HC}$ levels in hair, suggesting the existence of S-related ion channels [5] (designated as S or SO_4^{2-} channels).

Although channel gating produces a short pulsed inflow into the cell each time, the messenger protein binds with one of the associated receptors; such gating can occur so frequently as to bring the intracellular ion concentration $[X]_{CI}$ to serum ion concentration $[X]_I$. Since the $[X]_{CI}$ is kept at the serum $[X]_I$ by the channels' flow, $[X]_{HO}$ is determined by $[X]_I$ (see **Table 1**).

In HM cells, Ca can enter primarily as ionic ($[\text{Ca}]_{CI}$) with few protein-bound atoms ($[\text{Ca}]_{CP} = 0$). The cellular Ca concentration $[\text{Ca}]_C$ is equal to cell ion concentration $[\text{Ca}]_{CI}$, that is, $[\text{Ca}]_C = [\text{Ca}]_{CI}$. Ca is incorporated as a pair of atoms into the hair protein molecules formed in the HM cells [29]. The reaction rate of the pair formation is proportional to the

ion collision probability, $\{[Ca]_{CI}\}^2$, in the HM cell. The dissociation rate of two Ca pair atoms in the protein is proportional to twice the $[Ca]_H$. $[Ca]_H$ is in equilibrium with cell $[Ca]_C$; the rates are equal, $2r[Ca]_H = q\{[Ca]_{CI}\}^2$, where r and q are the proportional constants. When the channel gating frequency is high enough to result in $[Ca]_{CI} = [Ca]_I (=10)$, we have $[Ca]_{HO} = 50$. Therefore, $q = r$ and $[Ca]_{HO} = (1/2)[Ca]_I^2$. For a channel gating frequency, we can express as.

$$[Ca]_H = (1/2)[Ca]_{CI}^2.$$

Sr is assumed to be distributed equally as ion and protein-bound atom in HM cells, as established previously, that is, $[Sr]_{CI} = [Sr]_{CP}$. Similarly, we have

$$[Sr]_H = (1/2)\{[Sr]_{CI} + [Sr]_{CP}\}^2.$$

According to the definition $[X]_H = P/S$ by Eq. (2), the congener proportionality is expressed as $[Ca]_{CI} = [Sr]_{CI} = [Sr]_{CP}$, and the Sr/Ca ratio becomes $[Sr]_H/[Ca]_H = 4$. This agrees with experimental results (see **Figure 1**).

As seen above, when Ca channel gating takes place, the $[Sr]_H/[Ca]_H = 4$. For Ca channel closing, only the Ca and Sr on serum protein are incorporated into HM cells, resulting in $[Sr]_H = [Ca]_H = 10$ by Eqs. (9) and (11), $[Sr]_H/[Ca]_H = 1$. Thus, in this work, $[Sr]_H$ is a useful marker for channel gating.

Here, we first consider the hair elements without pollution. For dried serum from Ca-supplemented five male and five female subjects, a single concentration value for each element in **Table 1** was found. Ca appears to be the central and overriding player in the regulation of various elements; by ensuring normal serum Ca with a Ca supplement, all other elements under renal control (Sr, Cl, Br, K, S, P) become normal [5]. We have the Ca standard

$$[Ca]_S = [Ca]_I + [Ca]_P = 20 \text{ and } [Ca]_P = [Ca]_I = 10 \text{ (Dried serum)}$$

$$[Ca]_H = [Ca]_P = (1/2) [Ca]_S = 10 \text{ (Hair)}$$

with closed Ca channels (only serum protein can enter the HM cells, so $[Ca]_H$ must be equal to $[Ca]_P$ in steady-state hair growth).

Unfortunately, almost all humans have “ordinary deficiencies” in Ca in varying degrees [30, 31]. Calcium balance is maintained in kidney; Ca is freely filtered by the glomerulus, and the quantity of Ca filtered each day of over 10 g is far greater than the content of the entire ECF compartment [20]. Therefore, ~98% of the filtered Ca must be reabsorbed along the renal tubule. Approximately 70% of filtered Ca is reabsorbed passively in the proximal tubule. The remaining reabsorption is controlled by the Ca-sensor, CaSR, on the basolateral membrane of the tubular cells. Consequently, we have a tendency to fall into Ca deficiency. The ranges of $[Ca]_H < 10$ and $[Ca]_H > 10$ are due to Ca deficiency with deviations toward acidosis $[Cl]_H > 10$ and alkalosis $[Cl]_H < 10$, respectively. Two kinds of known Ca channels account for the results seen in hair analysis; the store-operated channel and PTH-operated channel are activated in the ranges of $[Ca]_H \leq 10$ and $[Ca]_H > 10$, respectively.

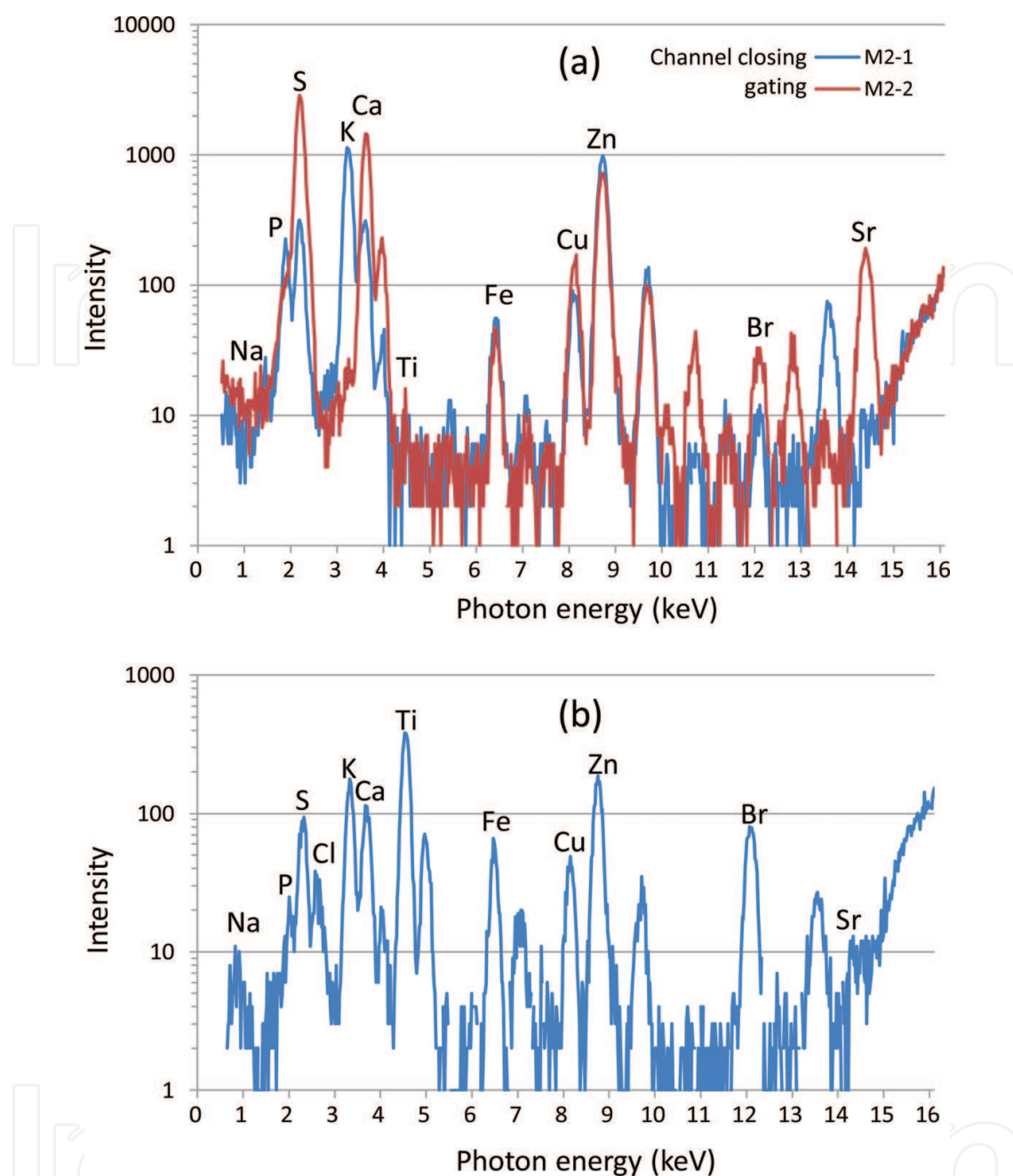


Figure 2. X-ray fluorescence spectra of single hair samples. (a) With ion channel closing and gating of Ca, K and S (SO_4^{2-}) in the hair matrix cells without pollution. Compare the peak heights with the levels listed in **Table 1**. (b) Typical example of hair with the pollution (F150 in **Figure 5**) showing a very high Ti peak and clearly recognized Na peak [Compare with (a)]. The [Ca] is lower than the normal, with store-operated Ca channel gating. The k-alpha peaks are labeled (see Section 2) (16.5–17.5 keV omitted to preserve useful scale).

Figure 1 gives a typical example showing the effects of both the store-operated and PTH-regulated Ca channels. The single strand from a 62-year-old female was analyzed from root to tip with the 0.05-mm-width excitation beam. As time progresses from right to left, the Ca deficiency is improving; the high-level $[\text{Ca}]_{\text{H}} = 50$ ($[\text{Sr}]_{\text{H}} = 200$) continues for a long term (12 months) from the tip, with deviations downward, keeping $[\text{Sr}]_{\text{H}}/[\text{Ca}]_{\text{H}} = 4$ and then abruptly

decreases to the low-level $[Ca]_H = 10$ standard, with $[Sr]_H/[Ca]_H = 1$ due to Ca channel closing, for about 2 months. Furthermore, the standard $[Ca]_H = 10$ is maintained for about 1.5 months by gating the store-operated Ca channels (SOCE) with $[Sr]_H/[Ca]_H \sim 2$; $[Ti]_H$ is as high as $[Ti]_H \sim 10$, with open Cl channels $[Cl]_H = [Br]_H = 22$ (acidosis: DA type). At the follicle (root), the concentrations become singular values, which will be reported elsewhere.

The observed process can be divided into three regions by the abrupt Sr change; the regions labeled "SOCE," DA-EE type with Ca channel closing, and "PTH regulated Ca entry." The store-operated Ca entry (SOCE) channel system is for maintaining the intracellular Ca at the normal by channel gating when the depletion of Ca storage in the cell occurs. For hair, therefore, the store-operated Ca channels must work for $[Ca]_H \leq 10$ so as to keep the normal $[Ca]_H = 10$, as reported earlier [6]. In contrast, the "PTH-regulated Ca entry" region indicates greater inflow of Ca and Sr through the gating Ca channels; the electrical signal initiated by the activation of the receptor PTH1R propagates rapidly over the surface of the cell due to the opening of other ion channels that are sensitive to the voltage change caused by the initial channel opening, as observed for renal epithelial Ca channel (TRPV5) as a typical example by de Groot et al [19]. For the hair Ca level, the channel gating frequency depends on serum [PTH] and causes the downward deviations from $[Ca]_H = 50$ and $[Sr]_H = 200$. Based on such results, the deduced type of Ca channel is referred to as "PTH-regulated Ca channels." Typical XFA spectra in **Figure 2(a)** show Ca channel closing and opening (gating) accompanied by levels changes for P (HPO_4^{2-}), S (SO_4^{2-}) and K^+ .

By taking into account, both the PTH-regulated and store-operated Ca channels, Ca deficiency can be classified into five distinct types, as summarized in **Table 2**. These five types describe the Ca patterns typical in the region before PM pollution was notable.

DE type has Ca deficiency for excitation of the PTH-regulated Ca channel gating resulting in a high-level $[Ca]_H > 10$ due to the Ca^{2+} inflow into HM cells.

The Ca^{2+} and Sr^{2+} inflow through the gating channels may become toxic [30, 31], resulting in abnormally high $[Cu]_H$ and/or $[Ti]_H$ and the inequality $[Cl]_H < [Br]_H$ (disordered chloride shift), which can be taken as the deterioration of hepatocytes and erythrocytes, respectively. In **Figure 1**, when the PTH-regulated Ca channels are closed, $[Cu]_H$ and $[Cl]_H$ become normal for the EE-type ($[Cu]_H = 10$, $[Cl]_H = 10$). In the store-operated SOCE region, the $[Ti]_H$ is high, that is, $[Ti]_H \sim 10$ (for normal $[Ti]_H \sim 1$), suggesting deterioration of Ti excretion as a consequence of Sr inflow into hepatocytes.

When the gating accumulates $[Ca^{2+}]$ and $[Sr^{2+}]$ to ionic serum levels in HM cells, that is, $[Ca]_{CI} = [Ca]_I = 10$ and $[Sr]_{CI} = [Sr]_I = 10$, we have the maximum $[Ca]_{HO} = 50$ and $[Sr]_{HO} = 200$ in **Table 1**. An 8-month lasting $[Ca]_{HO} = 50$ was observed for chronic Ca deficiency [6], as referred to as LD type (long-term Ca deficiency). "LD type" often causes fatty liver [31].

DO type (Ca deficiency with Overplus in serum) has Ca channels closed in $[Ca]_H > 10$ by an increase of serum $[Ca^{2+}]$ with bone resorption [22, 30, 31], which results in serum alkalosis accompanied by a high $[Ca]_P$ ($= [Ca]_H > 10$ for closed Ca channels). Consequently, we have $[Ca]_H = [Sr]_H > 10$ with $[Cl]_H = [Br]_H < 10$. In this case, the serum [PTH] becomes so low as to result in a high $[K]_H$ and a low $[S]_H$ ([5]. Also, see Section 5.2.)

LD type: Long-term continuation of DE type due to chronic Ca deficiency.

DE type: PTH-regulated Ca channel gating.

$$10 < [\text{Ca}]_{\text{H}} \leq 50 \text{ with } [\text{Sr}]_{\text{H}}/[\text{Ca}]_{\text{H}} = 4.$$

Ca (Sr) inflow into cells deteriorates their functions:

$[\text{Cu}]_{\text{H}} > 10$ and/or high $[\text{Ti}]_{\text{H}}$ by deteriorated metal excretion in hepatocytes.

$[\text{Cl}]_{\text{H}} > [\text{Br}]_{\text{H}}$ or $[\text{Cl}]_{\text{H}} < [\text{Br}]_{\text{H}}$ by deteriorated chloride shift in erythrocytes

PTH inhibits H^+/Na^+ -exchange and Na^+ -anion cotransport in renal tubule:

high $[\text{H}^+]$ in serum, K^+/H^+ exchange in cells, and $[\text{K}]_{\text{H}} \lesssim 10$.

low $[\text{SO}_4^{2-}]$ in serum, $[\text{S}]_{\text{H}} = 200$ by gating sulfate ion channels Eq. (8).

Serum: $[\text{Ca}]_{\text{I}} \lesssim 10$ and $[\text{Ca}]_{\text{P}} \lesssim 10$. High [PTH]. Acidosis.

DO type: PTH-regulated Ca channel closing with bone resorption by Ca deficiency.

$$[\text{Ca}]_{\text{H}} = [\text{Sr}]_{\text{H}} \gtrsim 10 \text{ with } [\text{Cl}]_{\text{H}} = ([\text{Br}]_{\text{H}}) < 10 \text{ (Alkalosis), } [\text{K}]_{\text{H}} = 200, [\text{S}]_{\text{H}} = 20.$$

Ca in serum protein increases with the alkalosis ($[\text{Ca}]_{\text{H}} = [\text{Ca}]_{\text{P}}$).

Serum: $[\text{Ca}]_{\text{I}} > 10$ and $[\text{Ca}]_{\text{P}} > 10$. [PTH]-0. Highly alkalosis.

EE type: Ever closing of Ca channels by Ca sufficient "Ever Enough". (No deficiency).

$$[\text{Ca}]_{\text{H}} = [\text{Sr}]_{\text{H}} = 10, [\text{Cl}]_{\text{H}} = ([\text{Br}]_{\text{H}}) \lesssim 10, [\text{K}]_{\text{H}} = 200, [\text{S}]_{\text{H}} = 20, [\text{P}]_{\text{H}} \gtrsim 10.$$

Serum: $[\text{Ca}]_{\text{I}} = 10$ and $[\text{Ca}]_{\text{P}} = 10$. [PTH]-0. Slightly alkalosis.

DA type: PTH-regulated Ca channel closing and Store-operated channel gating.

$$[\text{Ca}]_{\text{H}} = 10 \text{ with } 1 < [\text{Sr}]_{\text{H}}/[\text{Ca}]_{\text{H}} \leq 4 \text{ and } [\text{Ca}]_{\text{H}} < 10 \text{ with } [\text{Sr}]_{\text{H}}/[\text{Ca}]_{\text{H}} = 4.$$

($[\text{Cu}]_{\text{H}} = 10, [\text{Cl}]_{\text{H}} > 10, [\text{Ti}]_{\text{H}}$: high)

PTH inhibits H^+/Na^+ -exchange and Na^+ -anion cotransport in renal tubule:

high $[\text{H}^+]$ in serum, K^+/H^+ exchange in cells, and $[\text{K}]_{\text{H}} \lesssim 10$.

low $[\text{SO}_4^{2-}]$ in serum, $[\text{S}]_{\text{H}} = 200$ by gating sulfate ion channels Eq. (8).

Serum: $[\text{Ca}]_{\text{I}} \lesssim 10$ and $[\text{Ca}]_{\text{P}} \lesssim 10$. Mean [PTH]. Acidosis.

Table 2. Classification of Ca deficiency observed in hair with Eqs. (2) and (3).

In summary, for $[\text{Ca}]_{\text{H}} > 10$, hair Ca is by PTH-regulated Ca channels, DE for gating and DO type for closing.

At $[\text{Ca}]_{\text{H}} = 10$, if the normal state of $[\text{Ca}]_{\text{H}} = [\text{Sr}]_{\text{H}} = 10$ continues steadily, we can call this EE type (Ca ever enough to close Ca channels). Some healthy subjects have been found to keep EE type more than several months.

Usually, however, transitions between open and closed Ca channels occur at $[\text{Ca}]_{\text{H}} = 10$, resulting in $1 < [\text{Sr}]_{\text{H}}/[\text{Ca}]_{\text{H}} < 4$. Scanning the 50- μm width X-ray beam along the hair, in earlier work [6], we observed the $[\text{Ca}]_{\text{H}}$ maintained at $[\text{Ca}]_{\text{H}} = 10$ (normal) during the variation of the $[\text{Sr}]_{\text{H}}$ by Ca channel gating. Therefore, the observed Ca channel gating is due to some kind of store-operated type to be activated at $[\text{Ca}]_{\text{H}} = [\text{Ca}]_{\text{P}} \leq 10$. It was concluded that transition between $[\text{Ca}]_{\text{I}}$ -sensitive (PTH-regulated) and $[\text{Ca}]_{\text{P}}$ -sensitive (store-operated) channel gating occurs at $[\text{Ca}]_{\text{H}} = 10$.

In $[Ca]_H < 10$, the subjects have store-operated Ca channel gating with $[Sr]_H/[Ca]_H = 4$ (DA type). In this case, PTH-regulated channels are closed, and the hair Ca is due to Ca bound on serum protein, that is, $[Ca]_H = [Ca]_P < 10$. If the serum [PTH] is still high enough to inhibit the H^+/Na^+ exchangers from excreting H^+ in renal proximal convoluted tubular cells [32], serum $[H^+]$ increases; this deviation of serum pH toward acidosis ($[Cl]_H = [Br]_H > 10$ “DA type) ionizes the protein-bound Ca to increase serum $[Ca^{2+}]$. Therefore, Ca in serum protein is a stockpile that the body can tap in cases of Ca deficiency. Oral calcium supplementation shows no immediate effects on $[Ca]_H < 10$ and $[Sr]_H/[Ca]_H = 4$ (2-month Ca supplementation is needed).

Normally, molecular pumps on cell membrane expel Ca^{2+} ions (closing the Ca channels) so that the intracellular $[Ca^{2+}]$ is nearly zero. This creates a state for signal Ca^{2+} inflow through the associated channels. However, when Ca^{2+} stores are depleted at the endoplasmic reticulum (ER), the store-operated Ca channels open [17, 18, 33], as Cahalan [16] illustrated clearly; STIM proteins in the ER open the store-operated “Orai” Ca^{2+} channels and inhibit voltage-gated $Ca_v1.2$ channels in plasma membrane. Because of the ubiquitous Ca-sensing STIM proteins, this store-operated Ca channel gating may be assumed to be similar to that we observed in the hair [5, 6]. Then, Ca depletion in the ER likely occurs with the depletion of the Ca stored on serum proteins ($[Ca]_P = [Ca]_H < 10$ with closed PTH-regulated Ca channels).

By 2-month supplementation of Ca 900 mg/day (3ACa) [34], LD type recovers to DO to DA type; the level of Ca deficiency is in the decreasing order of LD, DE, DO, and DA (see **Table 2**).

4. Hair elements with minor effects of air pollution before 2009

In Japan, notable air pollution had not been frequent until 2009. **Figure 3** shows results from hair samples obtained before 2009, and elemental concentrations evaluated for the hair roots of 50 randomly selected subjects of each sex between their 30s and 70s; the labels’ Roman numerals stand for each age period, and the bar graph is in order of age.

By the criteria listed in **Table 2**, we can determine the type of each subject in **Figure 3** as labeled in **Figure 3(b)**. Examining **Figure 3(a)** and **(b)**, the high $[Cu]_H$ and $[Ti]_H$ are parallel with Sr-indicated gating ($10 < [Ca]_H \leq 50$ with $[Sr]_H/[Ca]_H = 4$), and thus related to opening of PTH-regulated Ca channels (DE type) causing deterioration of hepatic Cu and Ti excretion. Similar results can be seen for some DA-type subjects indicated by “LD-DA,” which are the DA type with $[Ca]_H < 10$ with $[Cl]_H > 10$ at present and were LD type in past. This means that recovery from Ca entry takes a long time. There are also many intrinsic DA-type subjects ($[Ca]_H < 10$ with $[Cl]_H > 10$) having the normal Cu level. Many have $[Sr]_H/[Ca]_H = 4$ by the opening of store-operated Ca channels.

In this way, we obtained the results showing all the subjects with Ca deficiency in varying degrees; 24 out of 50 are DA type, 20 are DO type, and 4 are DE type, 2 are LD-DA type for the male, and 31 out of 50 are DA type, 9 are DO type, and 6 are DE type, 4 are LD-DA type for the female. This means that DA type, the least severe type of Ca deficiency, occurs in half of the subjects, regardless of gender. The second level in severity (and the second step in cases of

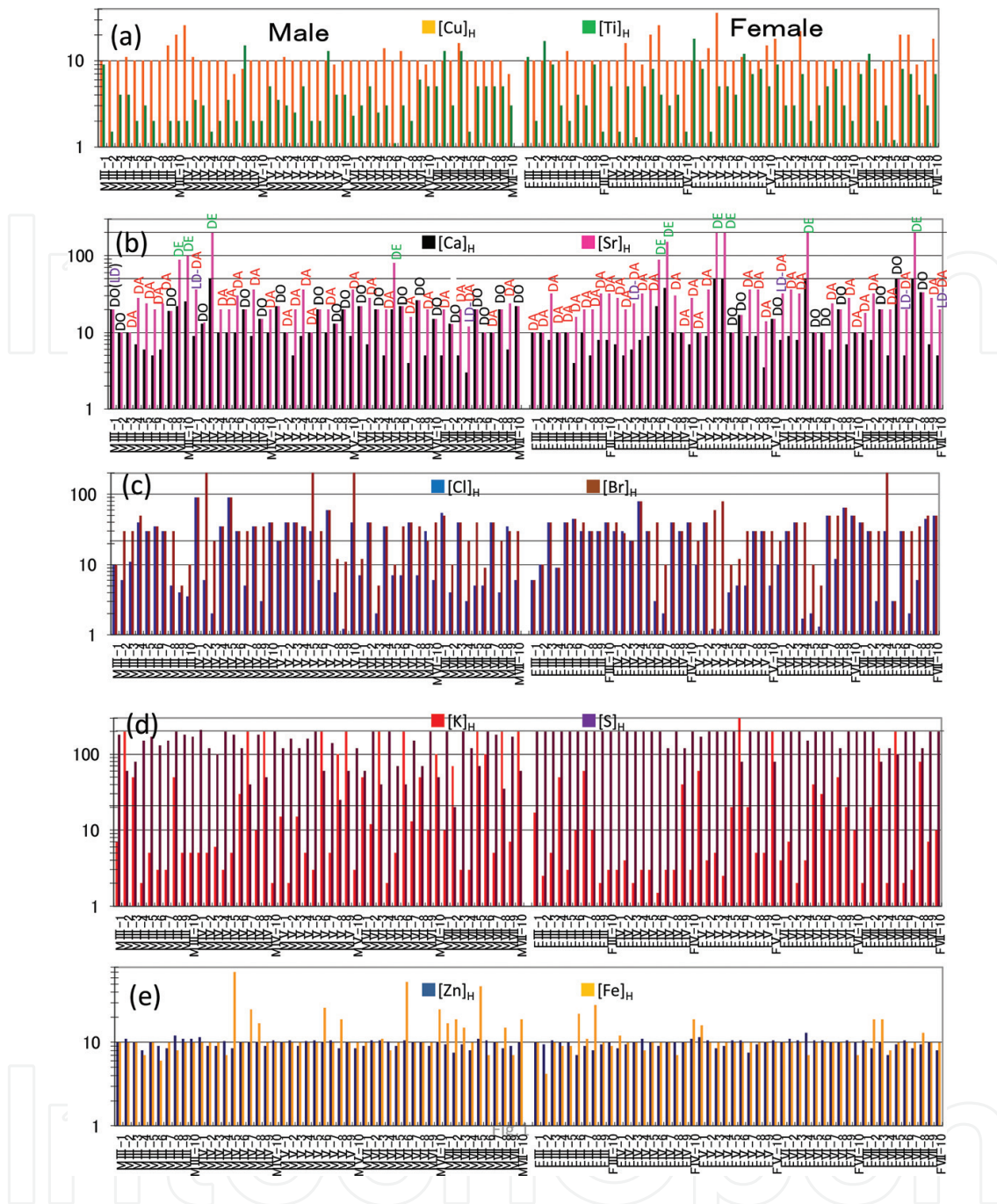


Figure 3. Hair concentrations observed for 50 randomly selected male and female subjects aged between 30 and 70. The hair samples were obtained before 2009 and show little or minor effects of air pollution. The bars graphed are in order of age and the Roman numerals in the subject labels stand for age period. (a) $[Cu]_H$ and $[Ti]_H$. The essential element Cu shows most values close to the homeostatic standard at $[Cu]_H = 10$ by Eq. (3), while Ti has a variety in $[Ti]_H$ by Eq. (2). (b) $[Ca]_H$ and $[Sr]_H$ having two separate standard levels with close and open Ca channels, $[Ca]_H = 10$ vs. $[Ca]_H = 50$ and $[Sr]_H = 10$ vs. $[Sr]_H = 200$, respectively. (c) $[Cl]_H$ and $[Br]_H$ having two separate standard levels at $[Cl]_H = [Br]_H = 10$ vs. $[Cl]_H = [Br]_H = 22$. (d) $[K]_H$ with the normal $[K]_H = 200$ and $[S]_H$ having two separate standard levels, $[S]_H = 20$ vs. $[S]_H = 200$. (e) $[Zn]_H$ and $[Fe]_H$ showing values close to the standard at $[Zn]_H = 10$ and $[Fe]_H = 10$ normalized by Eq. (3).

increasing deficiency), DO type, is more common for the male, and LD type is more common for the female, that is, the male appears to tolerate Ca deficiency by bone resorption, and the female by Ca channel gating.

In **Figure 3(d)**, almost all the females in our studies have the maximum $[S]_H = 200$ (SO_4^{2-} channel opening) due to Ca deficiency, and the normal $[S]_H = 20$ cannot be seen. For the males, $[S]_H$ values are slightly lower than the maximum, the two subjects MV-8 and MVII-2 (DO type) have the standard $[S]_H = 20$, and 10 subjects have the normal $[K]_H = 200$ (in DO type), which can be achieved by pumping K^+ into the HM cells with Na^+/K^+ -ATPase.

Figure 3(e) shows hair $[Zn]_H$ and $[Fe]_H$ for the same subjects. Zinc values are well regulated around the standard; $[Zn]_H$ is consistent with $[Zn]_H = [Zn]_S^2$. This implies that Zn atoms on the serum protein are incorporated into the hair protein in pairs, in the same manner as Ca (Ca in hair protein also exists as a pair of atoms) [5].

5. Air pollution observed by hair analysis in February 2011

The effect of air pollution on hair elements in Japan is discernible from 2009 onward. Especially, from February to March 2011, very high contents of Ti in hair were observed, as seen in **Figures 4–6**, corresponding to a period of yellow haze, and indicating PM from the mainland desert [35].

Figures 4 and **5** are from female subjects under 60 years old and above, respectively. **Figure 6** is from male subjects between 23 and 83. The bar graphs are in order of age. Almost all hair samples were taken in February 2011. Three-orders of magnitude higher $[Ti]_H$ can be seen. Such high levels of $[Ti]_H$ were also observed for hair samples obtained in Tokyo area in this period.

All the people in the area must have breathed the polluted air containing Ti. However, about 80% of the female subjects younger than 60 (**Figure 4**) have $[Ti]_H > 10$, and less than 30% of the male subjects showed this effect. **Figures 4–6(c)** show the $[Cl]_H$ and $[Br]_H$ for the same subjects. The correspondence between the high $[Ti]_H$ and high $[Cl]_H$ (and $[Br]_H$) is clear. The high $[Ti]_H$ should be attributed to the deterioration of the liver's function to excrete Ti into bile caused by Sr^{2+} inflow into hepatocytes. The $[Cl]_H$ abnormality can be attributed to Ca^{2+} inflow (in past) into erythrocytes through open Ca^{2+} channels (a PTH effect) ultimately caused by Ca deficiency. Recovery of Ca levels requires months of oral supplementation. Therefore, the observed $[Ti]_H$ and $[Cl]_H$ abnormalities mean that the affected subjects were LD type in past even if Ca is sufficient when the hair was taken. The observed difference between the sexes is due to most of the male subjects being DO type. Although all the subjects breathed the polluted air, the pollution effect depends on the Ca-deficiency history of the individuals. However, all elements Ca, Sr, Cl, Br, P, K, S, Cu, and Zn changed their levels in hair from those in **Figure 3**.

5.1. Store-operated Ca channel gating induced by the pollution

Ca contained in the polluted air, probably as calcium silicate, sulfate and carbonate, is breathed into the lung and must increase $[Ca^{2+}]$ in serum. As seen in **Figures 4–6(b)**, all the subjects have $[Ca]_H$ levels normal or less than the normal, that is, $[Ca]_H \lesssim 10$, except the subject labeled "F073" having parathyroid gland dysfunction. This means that PTH-regulated Ca channels are closed with the air pollution. Comparison with **Figure 3(b)** indicates that breathing the

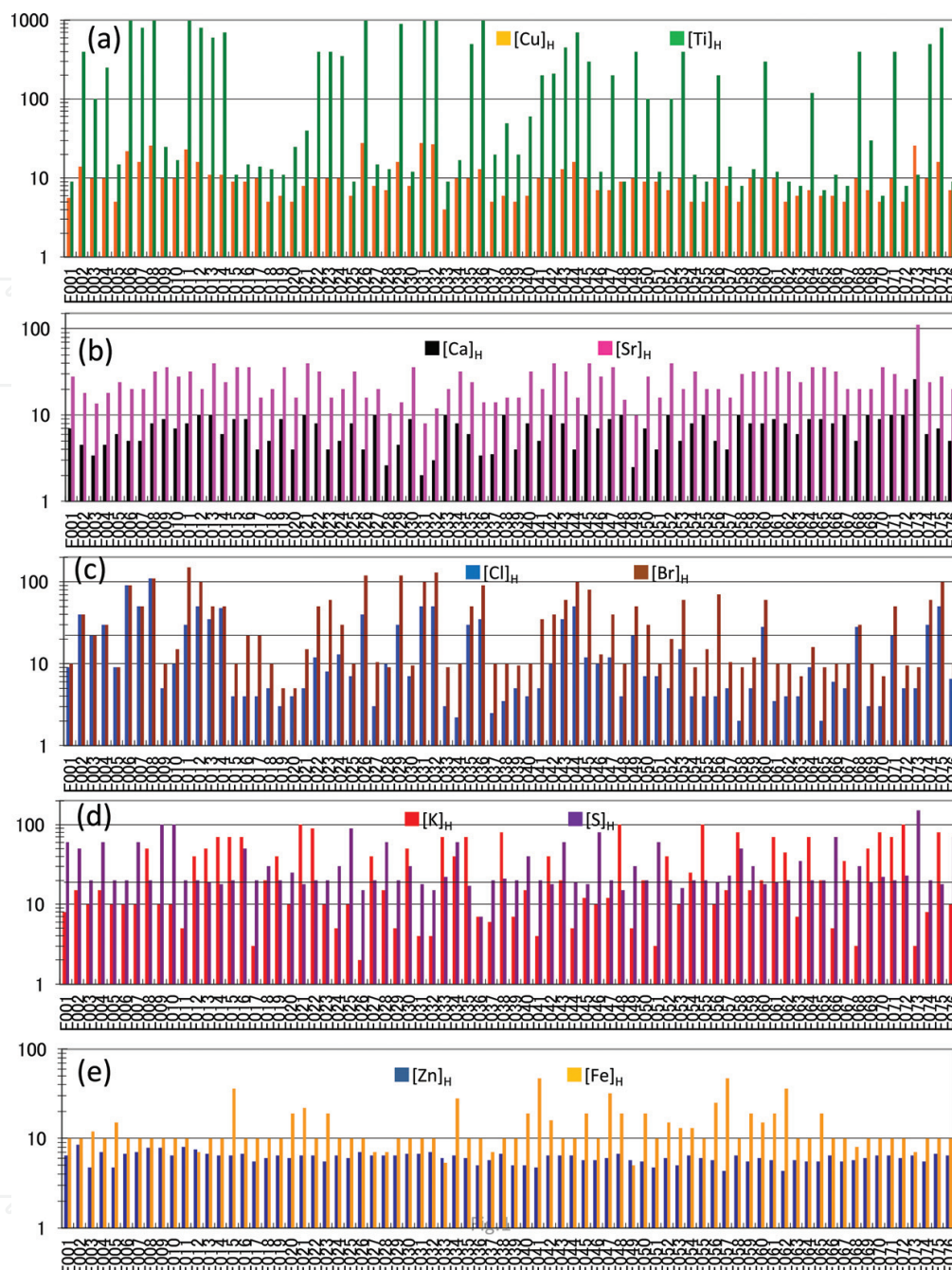


Figure 4. Effect of the air pollution on elements in hair root obtained in February 2011 from female subjects younger than 60. The bar graphs are in order of age from 23. Compare with **Figure 3**. (a) $[Cu]_H$ and $[Ti]_H$. Although the subjects younger than 42 (F019) have the normal $[Cu]_H = 10$ by Eq. (3), the $[Cu]_H$ level for the older is lower than the normal. The $[Ti]_H$ level by Eq. (2) is high for all the subjects; $[Ti]_H > 1000$ for the several subjects with the maximum of 2000 for F036 (age: 48), reflecting the atmosphere polluted with Ti. The high levels for $[Cu]_H$ and/or $[Ti]_H$ are consistent with deterioration of liver function. (b) $[Ca]_H$ and $[Sr]_H$. All the subjects have $[Ca]_H \leq 10$ due to PTH-regulated Ca channel closing except F073 (parathyroid gland dysfunction, $[Sr]_H/[Ca]_H = 4$ by PTH). (c) $[Cl]_H$ and $[Br]_H$. As a whole, $[Cl]_H$ (and $[Br]_H$) is lower than that for **Figure 3** by a deviation to alkalosis with a high $[Ca^{2+}]$ in serum. The very high $[Ti]_H$ in (a) is associated with the high $[Cl]_H$ ($[Br]_H$) (acidosis). (d) $[K]_H$ and $[S]_H$. Many subjects have the lower standard $[S]_H = 20$ with closing the ion channels attributable to breathing S in the polluted air. (e) $[Zn]_H$ and $[Fe]_H$ normalized by Eq. (3). All the subjects have low $[Zn]_H$ values (indicating 1/4 of the normal hair level), while the standard $[Fe]_H$ is seen for many subjects. The pollution effects shown here are for hair samples collected in Hyogo Prefecture. The similar effects are confirmed for those in Yokohama.

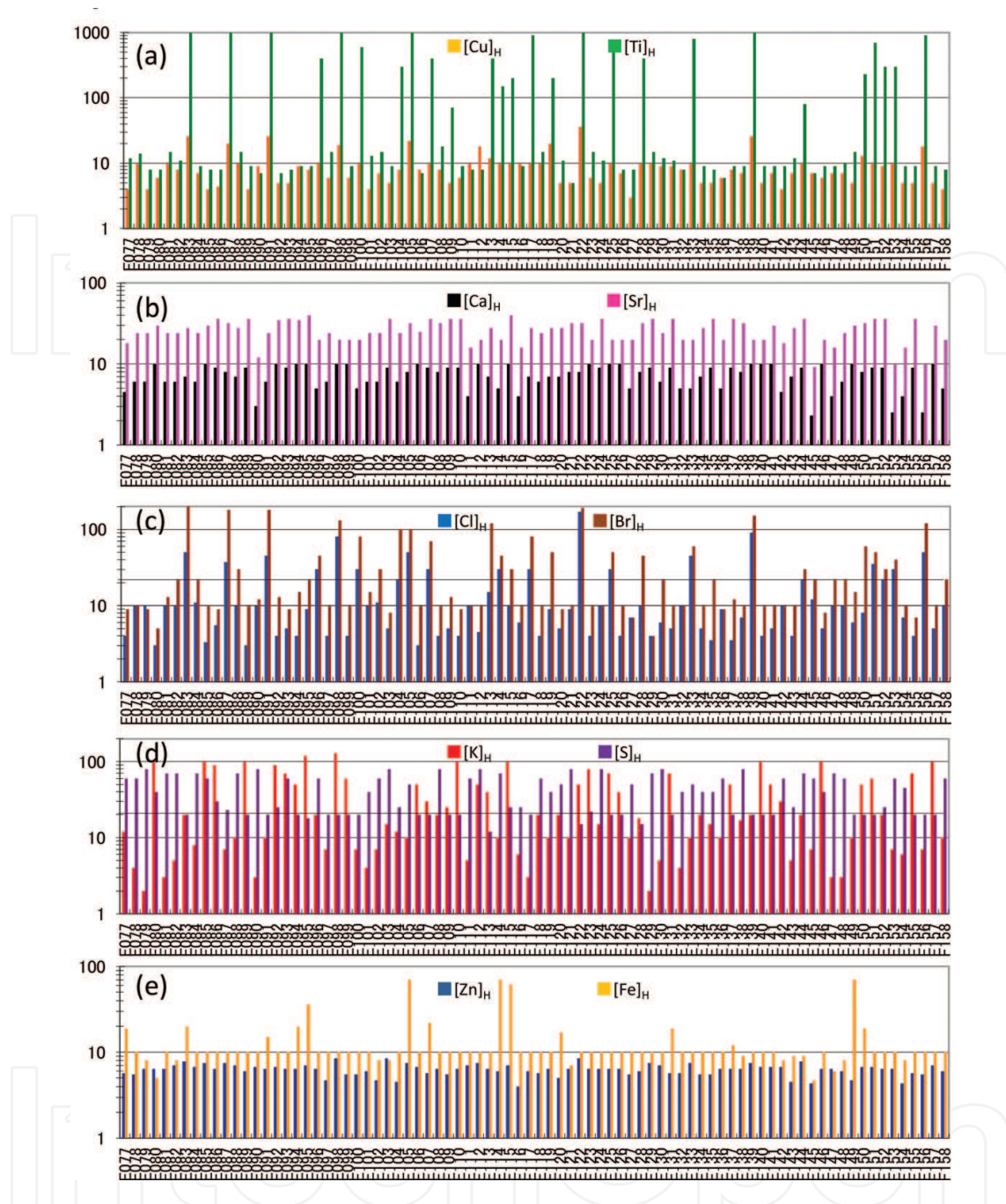


Figure 5. Effect of the air pollution on elements in hair root obtained in February 2011 from female subjects aged from 60 to 83. The bar graphs are in order of age. Compare with **Figure 3**. (a) $[Cu]_H$ and $[Ti]_H$. Almost all the subjects have $[Cu]_H < 10$ by Eq. (3). The $[Ti]_H$ level by Eq. (2) is high for all the subjects; $[Ti]_H > 1000$ for the several subjects with the maximum of 3000 for F122 (age: 69). (b) $[Ca]_H$ and $[Sr]_H$. All the subjects have $[Ca]_H \leq 10$ due to PTH-regulated Ca channel closing. (c) $[Cl]_H$ and $[Br]_H$. As a whole, $[Cl]_H$ ($[Br]_H$) is lower than that for **Figure 3** by a deviation to alkalosis with a high $[Ca^{2+}]$ in serum. Also, see the correspondence between very high $[Ti]_H$ in (a) and high $[Cl]_H$ ($[Br]_H$). (d) $[K]_H$ and $[S]_H$. The lower standard $[S]_H = 20$ is due to breathing S in the polluted air. (e) $[Zn]_H$ and $[Fe]_H$ normalized by Eq. (3). All the subjects have low $[Zn]_H$ values (1/4 of the normal), with the standard $[Fe]_H$ for many subjects.

polluted air (yellow sands) has an effect as if Ca supplements were taken. However, to increase Ca stored in serum protein to the normal $[Ca]_H = [Ca]_P = 10$, long-term Ca supplementation over 2 months with 900 mg/day is required. Therefore, the closing of PTH-regulated Ca

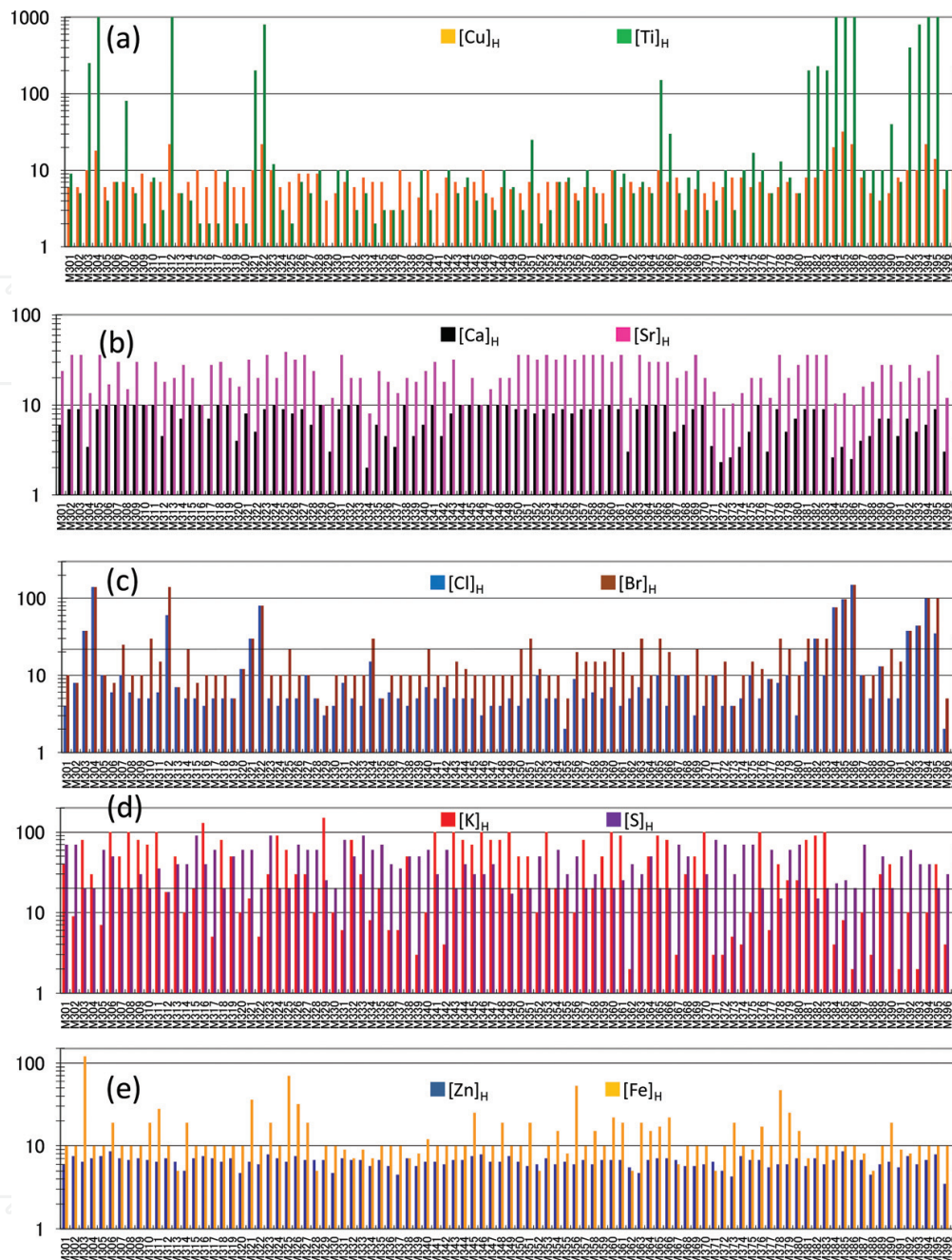


Figure 6. Effect of the air pollution on elements in hair root obtained in February 2011 from male subjects aged from 26 to 87. The bar graphs are in order of age. Compare with **Figure 3**. (a) $[Cu]_H$ and $[Ti]_H$. Almost all the subjects have $[Cu]_H < 10$ by Eq. (3). The high $[Ti]_H > 1000$ is seen for several subjects with the maximum of 3000 for M385 (age: 75). (b) $[Ca]_H$ and $[Sr]_H$. All the subjects have $[Ca]_H \leq 10$ due to PTH-regulated Ca channel closing. (c) $[Cl]_H$ and $[Br]_H$. As a whole, $[Cl]_H$ ($[Br]_H$) is lower than that for **Figure 3** by a deviation to alkalosis with a high $[Ca^{2+}]$ in serum. Also, see the correspondence between very high $[Ti]_H$ in (a) and high $[Cl]_H$ ($[Br]_H$). (d) $[K]_H$ and $[S]_H$. The lower standard $[S]_H = 20$ is due to breathing S in the polluted air. (e) $[Zn]_H$ and $[Fe]_H$ normalized by Eq. (3). All the subjects have low $[Zn]_H$ values (1/4 of the normal), with the standard $[Fe]_H$ for many subjects.

channels results in activation of the store-operated Ca channels; all the female subjects in **Figures 4** and **5** and almost all male subjects in **Figure 6** have $[Ca]_H < 10$ with $[Sr]_H/[Ca]_H = 4$ or $[Ca]_H = 10$ with $1 < [Sr]_H/[Ca]_H \leq 4$ produced by store-operated Ca channel opening. In other words, the pollution mainly changes the Ca channel gating into the store-operated type, which, if

this is by activation of the STIM proteins, inhibits voltage-gated Ca^{2+} channels ($\text{Ca}_v1.2$) responsible for activating heart muscle cells [33]. This may be taken as a risk factor for cardiovascular mortality (especially in cardiac patients) and to a lesser degree, for all persons.

5.2. Deterioration of molecular pumps in membrane by the pollution

Both the $[\text{K}]_{\text{H}}$ and $[\text{S}]_{\text{H}}$ for the same subjects are shown in **Figures 4–6(d)**. As seen in **Figure 3(d)**, almost all subjects without air pollution have low $[\text{K}]_{\text{H}} < 10$ and high $[\text{S}]_{\text{H}} = 200$ due to the PTH inhibition of both the excretion of H^+ (K^+/H^+ exchange in the cells) and the reabsorption of SO_4^{2-} in renal tubules, respectively [32]. The deficiency of SO_4^{2-} in serum causes ion channel gating into cells, through which SO_4^{2-} inflows into HM cells to give $[\text{S}]_{\text{H}} = 200$ (maximum by Eq. (8) in **Table 1**). However, the air pollution (apparently containing sulfur species) increases $[\text{SO}_4^{2-}]$ in serum in addition to the $[\text{Ca}^{2+}]$ increase as have been seen in **Figures 4–6(b)**, resulting in the lower level $[\text{S}]_{\text{H}} = 20$ due to ion channel closing. In **Figures 4–6(d)**, many subjects have the normal $[\text{S}]_{\text{H}} = 20$, which had been seldom seen without air pollution (before 2009) due to common dietary Ca deficiencies. We can conclude that the air pollution overfills $[\text{Ca}^{2+}]$ and $[\text{SO}_4^{2-}]$ in serum.

$[\text{K}]_{\text{H}}$ is proportional to the intracellular $[\text{K}]$, which strongly depends on K^+ transfer between cell and serum which is influenced by β -catecholamines, insulin, aldosterone, pH, and osmolality [36]. Each hair analysis gives the mean concentration for about 3 days (Section 2) and primarily shows the H^+/K^+ exchange depending on pH. In acidosis, H^+ ions move into cells and, to maintain electrical balance, K^+ ions move out into the serum, resulting in a low $[\text{K}]_{\text{H}}$, and vice-versa in alkalosis. The pollution increases the serum $[\text{Ca}^{2+}]$ and shifts the subject from acidosis to alkalosis. Therefore, there seen many high values of $[\text{K}]_{\text{H}}$ in **Figures 4–6(d)**. However, the $[\text{K}]_{\text{H}}$ values never reach the maximum level of $[\text{K}]_{\text{H}} = 200$ seen in **Figure 3(d)**. Since it is the maximum that is proportional to the serum $[\text{K}^+]$ [5], the $[\text{K}]_{\text{H}} \sim 100$ observed as the maximum indicates the serum $[\text{K}]_{\text{S}}$ at about a half of the normal, that is, hypokalemia defined as a $[\text{K}]_{\text{S}} < 3.5$ mmol/L, as opposed to the normal 5 mmol/L [23]. The maximum $[\text{K}]_{\text{H}} = 200$ can be reached by pumping K ions by the molecular pump, Na^+/K^+ -ATPase, which expels three sodium ions from the cell and takes in two potassium ions. If the pumping power deteriorates, therefore, the decrease of the $[\text{K}]_{\text{H}}$ maximum level must occur with an increase of $[\text{Na}]_{\text{H}}$. This can be seen in the typical example, **Figure 2(b)**, for a hair sample (F150) having a high $[\text{Ti}]_{\text{H}}$ from PM pollution; the Na $K\alpha$ peak at 1.04 keV appears clearly, in contrast to the nonpolluted samples in **Figure 2(a)**. Despite the high internal absorbance of sodium's 1.04 keV X-ray emission, such Na peaks were observed for many subjects in **Figures 4–6**. It may be concluded that the function of Na^+/K^+ -ATPase in cell membrane is deteriorated by the pollution.

Molecular ion pumps such as Na^+/K^+ -ATPase work with the energy supply of fully phosphorylated ATP. Therefore, serum $[\text{P}]$ is important in their deterioration. Both of P and Ca in serum are closely associated in an equilibrium relation with bone. The effect of the pollution on hair $[\text{P}]_{\text{H}}$ is seen in **Figure 7**; **Figure 7(a)–(d)** shows $[\text{P}]_{\text{H}}$ values observed for the hair samples in **Figures 3–6**. As has been reported [5], hair has the upper level of $[\text{P}]_{\text{H}} \gtrsim 10$ and lower level of $[\text{P}]_{\text{H}} = 5$ by Eq. (2). In **Figure 7(a)** without pollution, 12 out of 50 males and 7 out of 50 female subjects have the upper level $[\text{P}]_{\text{H}} \gtrsim 10$. Usually, $[\text{P}]_{\text{H}} < 5$ lower than the standard cannot be observed without air pollution [**Figure 7(a)**]. With the pollution, however, many hair samples

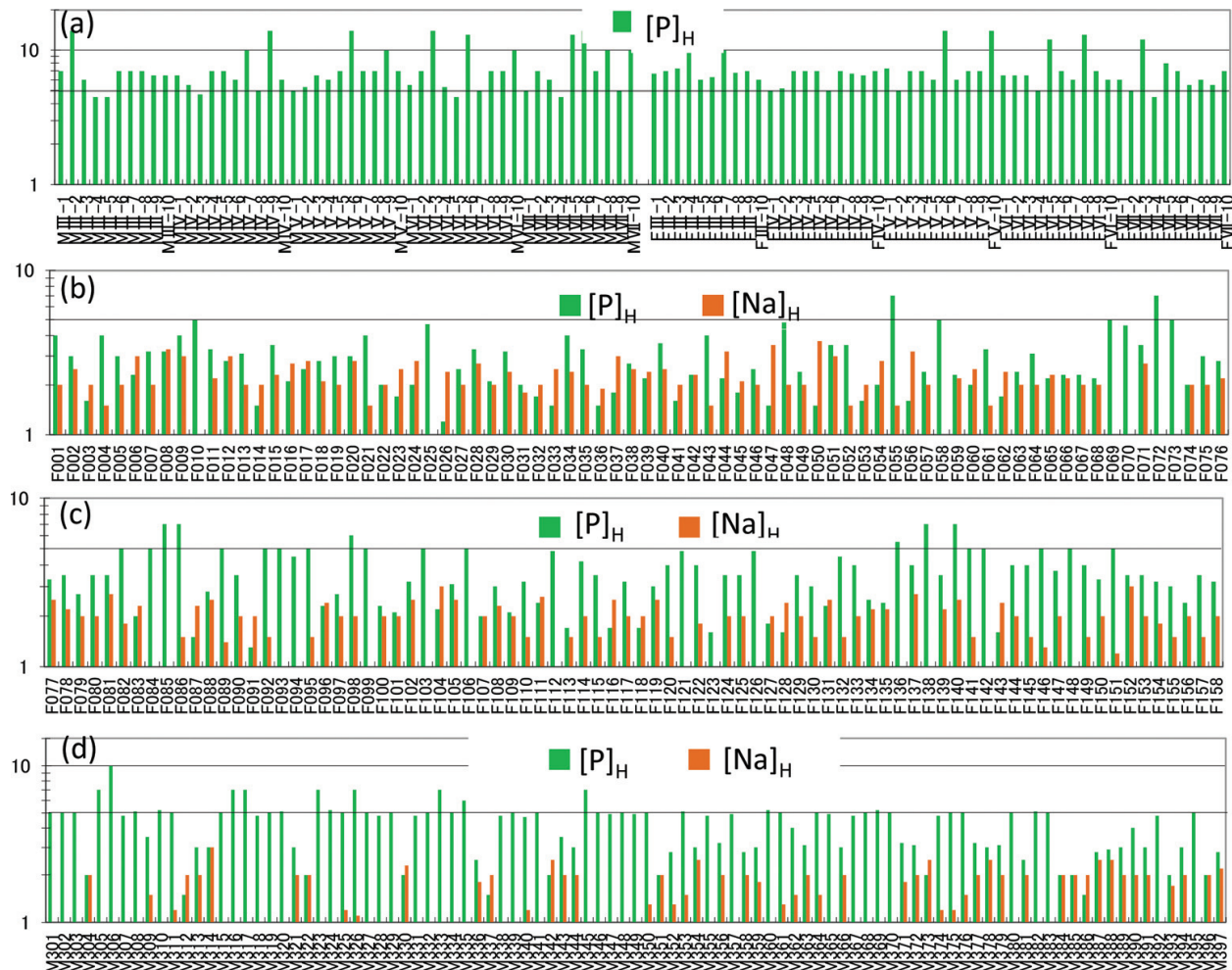


Figure 7. Association between $[P]_H$ and $[Na]_H$ with inactive Na^+/K^+ -ATPase due to the air pollution. (a) $[P]_H$ without air pollution for the male and female subjects in **Figure 3**. The upper and lower levels are seen at $[P]_H \geq 10$ and $[P]_H = 5$, respectively. $[Na]_H$ is not seen by the normal Na^+/K^+ -ATPase. (b) and (c) show $[P]_H$ and $[Na]_H$ for the female subjects in **Figures 4** and **5**, respectively. $[P]_H$ lower than the usual lower level is seen with the appearance of $[Na]_H$ peak. (d) $[P]_H$ for the male subjects in **Figure 6**; the low $[P]_H$ is accompanied by the $[Na]_H$ peak. The low $[P]_H$ values are often seen for the male over 60 (M351: 63). The abnormally low $[P]_H$ indicates insufficient energy supply to the Na^+/K^+ -ATPase. Breathing the polluted air increases serum $[\text{Ca}^{2+}]$ which moves to bone, accompanied by P to cause P deficiency.

in **Figure 7(b)–(d)** showed $[P]_H = 1.5\text{--}3.5$, much lower than the usual lower level. Also, the upper level $[P]_H \geq 10$ is not seen, except for the subject labeled “M306,” in **Figure 7(b)–(d)**. As a whole, $[P]_H$ is decreased by the air pollution; by Eq. (19) in **Table 1**, serum $[P]_I$ (HPO_4^{2-}) is calculated to be a half of the normal for $[P]_H = 3.5$ and $1/4$ for $[P]_H = 2.5$, taking $[P]_H = 5$ for the lower standard. This serum $[P]_I$ decrease may be explained as the pollution-induced excess Ca moving with P to bone by forming insoluble $\text{Ca} \times \text{PO}_4$; serum HPO_4^{2-} moving to bone must lower serum $[P]_S$ [20, 22, 32], and the deterioration of molecular pumps seems due to insufficient energy supply. Therefore, we can see the correlation between $[P]_H$ and $[Na]_H$; the low $[P]_H$ is accompanied by appearance of $[Na]_H$ peak as seen in **Figure 7(b)–(d)**. ($[Na]_H$ peaks were not seen in **Figure 7(a)** without pollution).

The serum [K] is regulated with free filtration at the glomerulus and by excretion-reabsorption in renal tubules. The reabsorption is produced by H^+/K^+ -ATPase [36] which is also deteriorated by the insufficient ATP supply, resulting in the hypokalemia understood from the hair level. This pollution's effect is serious; even mild or moderate hypokalemia increases the risks of morbidity and mortality in patients with cardiovascular disease [36, 37].

According to the meta-analysis for 57,158 patients with acute myocardial infarction (AMI) [37], primary ventricular fibrillation (PVF) is lethal and occurs without signs or symptoms of heart failure or cardiogenic shock. It was shown that patients with PVF had a lower serum K level before the event compared with patients without PVF. Though the weighted mean difference was small (-0.27 mmol/L), the finding of lower serum K before PVF was very consistent. The association between low [K] and PVF was confirmed in clinical settings. Patients with PVF have lower heart rates for inferior AMI and higher rates for anterior AMI. It can be concluded that the hypokalemia due to PM causes a mortality increase in AMI [25, 26] even 1 day after PM pollution increases. Also, it is well known that PVF results in blood stagnation in atrium to form clots having the risk for brain infarction.

The $[P]_H$ decrease as observed in **Figure 7** never takes place with oral Ca supplementation, which leads to the upper level $[P]_H \geq 10$ with $[Cl]_H = [Br]_H = 10$ [5]. The direct Ca intake by breathing the polluted air into the lung is essentially different from absorption through the GI tract and produces deficiency in the intracellular main ions [23], HPO_4^{2-} and K^+ .

In observation of [Na] and [P] by FXA, absorption of the Na $K\alpha$ and P $K\alpha$ by the specimen must greatly reduce the number of 1.04 and 2.01 keV photons reaching the detector. However, although low keV X-rays are received from only the hair surface, the calculation of concentration of P/S by Eq. (2) is valid because the absorption for the peak P and background S is produced by the same matrix. The observation of $[Na]_H$ increase and $[P]_H$ decrease is consistent with the emerging pattern and should not be dismissed because of the low sampling volume inherent.

5.3. Reduction of serum Cu and Zn with the pollution

Another effect of the pollution is the decrease of $[Cu]_H = [Cu]_S$ and $[Zn]_H = [Zn]_S^2$ [with the definition by Eq. (2)]. As seen from the comparison of **Figures 4–6(a)** and **(e)** with **Figure 3(a)** and **(e)** showing their normalized values by Eq. (3), most subjects have the normal $[Fe]_H = 10$ independent of pollution, but decreases of Cu and Zn, $[Cu]_H < 10$ and $[Zn]_H < 10$, are seen with the pollution. The $[Cu]_H$ decrease depends upon age, and many subjects older than 60 have $[Cu]_H = [Cu]_S < 5$ less than a half of normal. The $[Zn]_H$ decrease takes place about equally for the male and female populations studied. We estimate the average hair zinc level in **Figures 4–6(e)** to be 1/4 of normal, that is, the air pollution therefore decreases serum $[Zn]_S$ to half of normal by Eq. (6) in **Table 1**. The decrease in serum Cu and Zn may be due to S inflow into serum from air pollution, which then forms compounds such as CuS and ZnS which may be excreted from the liver and pancreas, respectively. Both Cu and Zn are essential elements. For Zn, the normal serum concentration is in the range of 0.08–0.15 mg/dL, and its lower limit is 0.06–0.07 mg/dL. A decrease by half is therefore dangerous.

Zinc serves as a structural center for maintaining the higher-order structure of protein. Zinc participates in the activity of more than 70 enzymes, including carbonic anhydrase (CA) and dehydrogenase. Almost all proteins related to gene expression contain Zn as a DNA-binding motif “zinc finger.” Zinc is essential for physiological functions such as growth, gestation, taste, and participates in immunity, brain development, insulin biosynthesis, and so on [38]. Therefore, the air-pollution’s effect on serum Zn is serious to many aspects of health.

The reduction of serum $[Cu]_S$ due to the pollution can also give an answer to the question of the increase of myocardial infarction mortality. It is firmly established that the formation of elastin protein, which gives elasticity to blood vessels, is copper-dependent [39–41], and Cu deficiency degenerates smooth muscle cells in the aortic walls. It was observed that elastin increases at the damage sites (scar) on aortic walls [41]. This indicates that elastin is necessary to correct damages, which, if unrepaired, trigger both aortic rupture and infarction. Therefore, the Cu deficiency due to PM can cause a mortality increase of myocardial infarction [25].

Here, it should be noted that we encountered many subjects having the normal $[S]_H = 20$ in **Figures 4–6(d)**, in contrast to **Figure 3(d)** showing $[S]_H = 200$. This observation indicates that the serum [S] remains normal by excreting the excess [S] incorporated from the pollution together with Cu, and Zn [implying the essentiality for some sulfur species, referred to as sulfate, having its own or accessible ion channels. See **Figure 2(a)**].

6. Differences in pollution effect between the sexes

The normal levels of hair elements are the same for male and female. However, the pollution effects show differences as seen clearly in **Figures 4–7**. As described in Section 4, male and female deal with Ca deficiency differently; DO type is more common for the male, and LD type is more common for the female, that is, males tolerate Ca deficiency with Ca channels closed by bone resorption, and females have a tendency to open the PTH-regulated Ca channels without bone resorption. The resulting Ca and/or Sr inflow through the channels causes deterioration of the hepatocytes’ function to excrete pollutants into bile; a dysfunction that persists for months. Consequently, the pollution effect appears greater for the female; more female subjects have the high $[Ti]_H$ as seen in **Figures 4–6(a)**.

In **Figure 7**, the appearance of $[Na]_H$ due to the excess serum Ca by breathing the polluted air shows difference between the sexes clearly; male can accommodate the excess Ca on serum protein as expected from the fact that DO type is more common for male.

The pollution’s effect to decrease $[Cu]_H$ and $[Zn]_H$ can be recognized in **Figures 4–6(a)** and **(e)**. However, no difference between the sexes is clear; this implies these elements have no relation to the Ca metabolism, suggesting an association with the excess [S] in serum due to the pollution. By forming sulfide species, zinc and copper are excreted mainly with pancreatic fluid and bile into the gut, respectively.

The observed relation between the sexes leads to the conclusion that the serum element levels change so as to eliminate the excess Ca and S inhaled from the air pollution.

7. Conclusion

Hair calcium depends on both PTH-regulated and store-operated Ca^{2+} channels; oral Ca supplementation transits hair Ca level from the Ca upper level ($[\text{Ca}]_{\text{H}} = 50$) to the lower level (normal $[\text{Ca}]_{\text{H}} = 10$) by closing PTH-regulated Ca channels of hair matrix cells (HM cells), and gives no effects on the store-operated channels which are activated by the decrease of stock Ca bound on serum protein. In-vitro studies ([16–18] show store-operated “Orai” Ca channels activate when Ca^{2+} stores are depleted at the endoplasmic reticulum (ER). Together with hair studies (in vivo), our analysis concludes that the store-operated and PTH-regulated Ca channels activate with depletion of $[\text{Ca}]_{\text{P}}$ and $[\text{Ca}]_{\text{I}}$ in Eq. (1), respectively, both of which are regulated by PTH.

Without air pollution before 2009, a half of the 100 subjects were classified as mildly calcium-deficient DA type ($[\text{Ca}]_{\text{H}} = [\text{Ca}]_{\text{P}} < 10$ with $[\text{Cl}]_{\text{H}} > 10$), and the other half are of more severe Ca deficiency related to PTH-regulated Ca channels ($[\text{Ca}]_{\text{I}} < 10$).

The air pollution from February to March 2011 overfilled Ca ($[\text{Ca}^{2+}]$) and S ($[\text{SO}_4^{2-}]$) in serum. Consequently, except one patient with parathyroid gland dysfunction, all the subjects had the normal or lower $[\text{Ca}]_{\text{H}} \lesssim 10$ (with $[\text{Cl}]_{\text{H}} < 10$) produced by closed PTH-regulated Ca channels, and almost all the subjects had store-operated Ca channel gating, which, if done by the STIM proteins, inhibits voltage-gated Ca channels and worsens cardiac risks.

The overfilled Ca and S in serum has consequences: we expect that Ca is removed as the phosphate to bone and S is removed to bile and pancreatic fluid as excretable metal sulfides, resulting in loss of needed Zn and Cu. Serum $[\text{K}]$ as well as $[\text{Cu}]$ and $[\text{Zn}]$ decrease to half of the normal level with air pollution. The excessive Ca^{2+} results in a notable deficiency of serum $[\text{P}]$. It must create a shortage of ATP, which deteriorates cell membrane molecular pumps such as H^+/K^+ -ATPase and Na^+/K^+ -ATPase, responsible for the renal K reabsorption, resulting in hypokalemia to produce fatal ventricular fibrillation in patients with myocardial infarction accompanied with heart rate variability [26]. It is well known that even mild or moderate hypokalemia increases the risks of mortality in patients with cardiovascular diseases. Abnormal intracellular $[\text{K}]$ and $[\text{Na}]$ due to the inactive molecular pumps may be also responsible for heart rate variability. (K^+ and Na^+ regulate and form the electric pulses commanding myocardial movement.)

The excessive $[\text{S}]$ in serum may decrease toward the normal by forming sulfide compounds with Cu and Zn, which are excreted from the liver and pancreas, resulting in deficiency of Cu necessary for the formation of elastin protein to repair damage in blood vessels. Thus, the sulfur species in the pollution may provide a second increase the mortality in myocardial infarction [25].

In summation, hair analysis shows that post-2009 air pollution causes serious deficiencies in serum K, P, Cu, and Zn, and is likely responsible for various diseases.

Finally, it is emphasized that the deterioration of Na^+/K^+ -ATPase (**Figure 7**) is a serious pollution effect because Na^+/K^+ -ATPase exists in all cells, for example, more than half of brain energy dissipation is due to Na^+/K^+ -ATPase; the pollution effect on neurodegenerative disease [42] is conceivable.

Acknowledgements

This work has been performed under the approval of the Photon Factory (Proposal No. 2005R15, 2006G408, 2009Y011, 2009Y022, 2010Y023) in collaboration with industry (Health Analysis Laboratory, Ltd.). The authors would like to express their sincere thanks to Professor A. Iida, Photon Factory, for his great help with the experiments at BL-4A. His sophisticated instrumentation made it possible to analyze the hair roots from thousands of people.

Author details

Jun-ichi Chikawa^{1*}, Jeremy Salter¹, Hiroki Shima², Takaaki Tsuchida³, Takashi Ueda⁴, Kousaku Yamada¹ and Shingo Yamamoto⁵

*Address all correspondence to: chikawa@hyogosta.jp

1 Hyogo Science and Technology Association, Himeji, Japan

2 Shima Institute in Quantum Medicine, Osaka, Japan

3 National Cancer Centre, Tokyo, Japan

4 Ueda Heart Clinic, Tatsuno-shi, Hyogo, Japan

5 Hyogo College of Medicine, Nishinomiya, Hyogo, Japan

References

- [1] Iida A, Noma T. Nuclear Instruments & Methods. 1993;**B82**:129-138
- [2] Ito A, Inoue T, Kawai T, Taki Y, Inoue S, Shimizu T, Shinohara K. AIP Conference Proceedings 1696. 020021-1-5; 2016
- [3] Noguchi T, Itai T, Kawaguchi M, Takahasshi S, Tanabe S. Applicability of human hair as a bioindicator for trace elements exposure. In: Kawaguchi M, Misaki K, Sato H, Yokokawa T, Itai T, Nguyen TM, Ono J, Tanabe S, editors. Environmental Chemistry. Vol. 6. Tokyo: Terra Scientific Publishing; 2012. pp. 73-77

- [4] Chikawa J, Yamada K, Akimoto T, Sakurai H, Yasui H, Yamamoto H, Okabe S, Ebara M. *Journal of X-Ray Science and Technology*. 2007;**15**:109-129
- [5] Chikawa J, Mouri Y, Shima H, Yamada K, Yamamoto H, Yamamoto S. *Journal of X-ray Science and Technology*. 2014;**22**:471-491
- [6] Chikawa J, Mouri Y, Shima H, Yamada K, Yamamoto H, Yamamoto S. *Journal of X-ray Science and Technology*. 2014;**22**:587-603
- [7] Dockery DW, Pope CA III, Xu X, Spengler JD, Ware JH, Fay ME, Ferris BG Jr, Speizer FE. *The New England Journal of Medicine*. 1993;**329**:1753-1759
- [8] Pope CA III, Thun MJ, Namboodiri MM, Dockery DW, Evans JS, Speizer FE, Heath CW Jr. *American Journal of Respiratory and Critical Care Medicine*. 1995;**151**:669-674
- [9] Pope CA III, Burnett RT, Thun MJ, Calle EF, Krewski D, Ito K, Thurston GD. *Journal of the American Medical Association*. 2002;**287**:1132-1141
- [10] Ueda K, Nitta H, Ono M, Takeuchi A. *Journal of the Air & Waste Management Association*. 2009;**59**:1212-1218
- [11] Creamean JM, Suski KJ, Rosenfeld D, Cazorla A, DeMott PJ, Sullivan RC, White AB, Ralph FM, Minnis P, Comstock JM, Tomlinson JM, Prather KA. *Science*. 2013;**339**:1572-1578
- [12] Goudie AS, Middleton NJ. *Desert Dust in the Global System*. Amsterdam: Springer; 2006
- [13] Grousset FG, Ginoux P, Bory A, Biscaye PE. Case study of a Chinese dust plume reaching the French Alps. *Geophysical Research Letters*. 2003;**30**:1277-1280
- [14] Husar RB, Tratt DM, Schichtel BA, Falke SR, Li F, Jaffe D, Gassó S, Gill T, Laulainen NS, Lu F, Reheis MC, Chun Y, Westphal D, Holben BN, Gueymard C, McKendry I, Kuring N, Feldman GC, McClain C, Frouin RJ, Merrill J, DuBois D, Vignola F, Murayama T, Nickovic S, Wilson WE, Sassen K, Sugimoto N, Malm WC. *Journal of Geophysical Research*. 2001;**106**:18317-18330
- [15] Fernandez TA, Casan CP. *Archivos de Bronconeumología*. 2012;**48**:240-246
- [16] Cahalan MD. *Science*. 2010;**330**:43-44
- [17] Park CY, Shcheglovitov A, Dolmetsch R. *Science*. 2010;**330**:101-105
- [18] Wang Y, Deng X, Mancarella S, Hendron E, Eguchi S, Soboloff J, Tang XD, Gill DL. *Science*. 2010;**330**:105-109
- [19] de Groot T, Lee K, Langeslag M, Xi Q, Jalink K, Bindels RJM, Hoenderop JGJ. *Journal of the American Society of Nephrology*. 2009;**20**:1693-1704
- [20] Favus MJ, Bushinsky DA, Lemann J Jr. Regulation of calcium, magnesium, and phosphate metabolism. In: Favus MJ, editor. *Primer on the Metabolic Bone Diseases and Disorders of Mineral Metabolism* (Chapter 13, 6th edition). American Society for Bone and Mineral Research: Washington, DC; 2006. pp. 76-83

- [21] Osaki T, Takeuchi S. *Analytical Chemistry*. 2017;**89**:216-231
- [22] Brown EM, Jüppner H. Parathyroid hormone: Syntheses, secretion, and action. In: Favus MJ, editor. *Primer on the Metabolic Bone Diseases and Disorders of Mineral Metabolism* (Chapter 15, 6th edition). Washington, DC: American Society for Bone and Mineral Research; 2006. pp. 90-99
- [23] Gamble JL. *Chemical Anatomy, Physiology and Pathology of Extracellular Fluid: A Lecture Syllabus*. Cambridge, MA: Harvard University Press; 1949
- [24] Kraut JE, Madias NE. *Clinical Journal of American Society of Nephrology*. 2007;**2**:162-174
- [25] Mustafic H, Escolano S, Empana P. *JAMA*. 2012;**307**:713-721
- [26] Pope CA III, Verrier RI, Lovett EG, Larson AC, Raizenne ME, Kanner RE, Schuwartz J, Villegas GM, Gold DR, Dockery DW. *American Heart Journal*. 1999;**138**:890-899
- [27] Pope CA III, Muhlestein JB, May HT, Renlund DG, Anderson JL, Horne BD. *Circulation*. 2006;**114**:2443-2448
- [28] Cornelis R, Fuentes-Arderiu X, Bruunshuus I, Templeton D. *Pure and Applied Chemistry*. 1997;**69**:2593-2606
- [29] Aksirov AM, Gerasimov VS, Kondratyev VI, Korneev VN, Kulipanov GN, Lanina NF, Letyagin VP, Mezentsev NA, Sergienko PM, Tolochko BP, Trounova VA, Vazina AA. *Nuclear Instruments & Methods*. 2001;**A470**:380-387
- [30] Fujita T. *Journal of Bone and Mineral Metabolism*. 1998;**16**:195-205
- [31] Fujita T, Palumieri GMA. *Journal of Bone and Mineral Metabolism*. 2000;**18**:109-125
- [32] Bringham FR. Physiologic actions of PTH and PTHrP II. Renal actions. In: Bilezikian JP, Marcus R, Levine MA, editors. *The Parathyroids, Basic and Clinical Concepts* (Chapter 14, 2nd edition). San Diego: Academic Press; 2001. pp. 227-243
- [33] Clapham DE. *Cell*. 2007;**131**:1047-1058
- [34] Fujita T. *Journal of Bone and Mineral Metabolism*. 1996;**14**:31-34
- [35] Zhang R, Shen Z, Cheng T, Zhang M, Liu Y. *Aerosol and Air Quality Research*. 2010;**10**:67-75
- [36] Greenlee M, Wingo CS, McDonough AA, Youn J-H, Kone BC. *Annals of Internal Medicine*. 2009;**150**:619-625
- [37] Gheeraert PJ, De Buyzere ML, Taeymans YM, Gillebert TC, Henriques JP, De Backer G, De Bacquer D. *European Heart Journal*. 2006;**27**:2499-2510. [PMID: 16952926]
- [38] Cunnane SC. *Zinc, Clinical and Biochemical Significance*. CRC Press; 1988
- [39] Miller EJ, Martin GR, Mecca CE, Piez KA. *The Journal of Biological Chemistry*. 1965;**240**:3623-3627

- [40] Prohaska JR, Heller L. *The Journal of Nutrition*. 1982;**112**:2142-2150
- [41] Wildgruber M, Bielicki I, Aichler M, Kosanke K, Feuchtinger A, Settles M, Onthank DC, Cesati RR, Robinson SP, Huber AM, Rummeny EJ, Walch AK, Botnar RM. Assessment of myocardial infarction and postinfarction scar remodelling with an elastin-specific magnetic resonance agent. *Circular Cardiovascular Imaging*. 2014;**7**:321-329
- [42] Kioumourtzoglou M-A, Schwartz JD, Weisskopf MG, Melly SJ, Wang Y, Dominici F, Zanobetti A. *Environmental Health Perspectives*. 2016;**124**:23-29

IntechOpen

